

Heatley Medal Lecture

What we have learned from ribosome structures

V. Ramakrishnan¹

MRC Laboratory of Molecular Biology, Hills Road, Cambridge CB2 0QH



Heatley Medal Lecture

Delivered at the University of Manchester
on 26 March 2008

V. Ramakrishnan

Abstract

The determination of the high-resolution structures of ribosomal subunits in the year 2000 and of the entire ribosome a few years later are revolutionizing our understanding of the role of the ribosome in translation. In the present article, I summarize the main contributions from our laboratory to this worldwide effort. These include the determination of the structure of the 30S ribosomal subunit and its complexes with antibiotics, the role of the 30S subunit in decoding, and the high-resolution structure of the entire 70S ribosome complexed with mRNA and tRNA.

Historical background

Ribosomes are large macromolecular assemblies consisting of approx. two-thirds by mass of RNA, with the rest being proteins. Given their molecular mass of approx. 2.5 MDa in bacteria, it was not clear whether it would ever be possible to determine their high-resolution structure.

By around 1980, several large complexes had been crystallized. The ribosome, however, was considerably larger than any of these; moreover, it was not even clear initially whether ribosomes in the cell were identical or consisted of a mixture of subtypes that might be specialized for different messages.

The finding that the large (50S) subunit from *Geobacillus stearothermophilus* (formerly *Bacillus stearothermophilus*) could yield true three-dimensional crystals was therefore a significant landmark [1]. A few years later, the crystallization

of both the small (30S) subunit and the entire 70S ribosome from *Thermus thermophilus* was also reported [2]. Thus, by the end of the 1980s, both subunits and the entire ribosome had been crystallized. These early crystals were not of sufficient quality to yield a high-resolution structure, since they generally diffracted to worse than 10 Å (1 Å = 0.1 nm) resolution. However, after an extensive search involving many different species, Yonath and co-workers reported that the 50S subunit from the archaeal species *Haloarcula marismortuii* could yield diffraction to 3 Å resolution [3], showing that it might be possible in principle to obtain a high-resolution structure that could be interpreted in molecular detail. The development of synchrotron radiation sources to provide intense beams of X-rays [4] was crucial to provide sufficient signal from these weakly diffracting crystals. Another advance was the development of cryocrystallography as a general tool to minimize radiation damage from these intense X-ray beams [5], which was quickly adapted for data collection on ribosomal crystals [6]. Advances in computing, detectors and crystallographic software were also essential.

Nevertheless, despite these advances, little progress was made through most of the 1990s in obtaining a structure even at the modest resolution of 6–10 Å that should have been technically feasible by that time. This situation began to change when the group at Yale showed that heavy-atom clusters could be seen directly in difference Patterson maps of the *H. marismortuii* 50S subunit at 9 Å resolution [7]. These heavy-atom positions were confirmed by difference Fourier maps using phases from molecular replacement starting with a cryo-EM (electron microscopy) map of the 50S subunit. However, it is not clear that an EM starting model was necessary, given the strong difference Patterson peaks present in the X-ray data. In any case, for the first time, right-handed helical density corresponding to A-form helices were observed in electron-density maps of a ribosomal subunit, demonstrating a feasible approach to initiating phasing for such large complexes. Our approach for the 30S subunit is outlined below.

The structure of the 30S subunit

Crystallography

When we began crystallographic studies on the 30S subunit, the best reported diffraction from crystals of this subunit

Key words: antibiotic, codon-anticodon pairing, decoding, ribosome, RNA, X-ray crystallography.

Abbreviations used: ASL, anticodon stem-loop; EM, electron microscopy.

¹email ramak@mrc-lmb.cam.ac.uk

was to approx. 7–8 Å resolution, and phasing to even lower resolution was presumably compromised by the fact that the space group assigned to those crystals was incorrect [8]. Our approach to this problem has been documented in detail elsewhere [9]. Briefly, our initial crystals of the 30S subunit from *T. thermophilus* were shown to lack ribosomal protein S1, which is present in variable stoichiometry in purified ribosomes and is not essential for poly(U)-directed poly-phenylalanine synthesis *in vitro*. The quantitative removal of this variable component produced large crystals more reliably, and these diffracted to a resolution of better than 3 Å.

Efforts to obtain a molecular-replacement solution using a cryo-EM map of the 30S subunit were not successful. It is not clear whether this was due to a slight difference in the absolute scale of the EM map or to the intrinsic conformational variability of the 30S subunit.

For phasing using heavy atoms, our previous work suggested that the signal-to-noise ratio from anomalous scattering was much greater than expected due to nearly perfect isomorphism and lack of scaling errors [10,11]. A common anomalous scatterer used for phase determination is selenium incorporated into proteins as selenomethionine [12]. For the 30S subunit, calculations showed that selenomethionine was not likely to be as useful an anomalous scatterer because the K edge of selenium has a peak height of f'' of only a few electrons, and ribosomal proteins are methionine-poor and in any case represent only a third of the total scattering mass. However, the LIII edge from elements such as lanthanides, tungsten or osmium can have a peak height of f'' of as much as 20 electrons [13,14]. In particular, previous work on the P4–P6 domain of the group I intron showed that osmium hexammine was likely to be a particularly suitable compound for phasing crystals of large RNAs [14] because osmium has a large anomalous LIII edge, and the nature of the compound's binding site in RNA suggested that there would be a sufficient number of sites in a ribosomal subunit.

In our initial phasing of 30S diffraction data, we employed anomalous scattering from the LIII edges of not only various known heavy-atom clusters of tungsten and tantalum, but also salts of lanthanides and osmium hexammine [15]. Subsequently, test phasing runs showed that osmium hexammine alone would have provided phases that were as good as the combined phases; moreover, the heavy-atom positions could be determined by automated methods such as the program SOLVE [16]. Indeed, anomalous scattering from this compound or the closely related iridium hexammine proved essential for the phasing of the high-resolution 50S structure [17] as well as a lower-resolution structure of the entire 70S ribosome [18].

This phasing strategy led to 5.5 Å maps of the 30S subunit, where, for the first time, we could see right-handed double-helical RNA in which individual backbone strands and even bumps for individual phosphate groups could be discerned. At this resolution, it was also possible to see individual α -helices of proteins, and thereby fit proteins of known structure into the maps of the 30S subunit. This, in combination with a vast body of biochemical data on the ribosome, allowed

us to approximately model about a third of the subunit, including almost the entire central domain of 16S RNA.

The determination of phases to higher resolution was not entirely straightforward owing to a combination of crystal-to-crystal non-isomorphism and radiation damage [9], but the remaining problems were overcome within a year, and an essentially complete atomic model of the 30S subunit refined to 3 Å resolution was published [19]. The structure consists of 20 polypeptide chains (S2–S20 and a small peptide called THX) and over 1500 nucleotides of 16S RNA (Figure 1). Some features of the structure are immediately noticeable. The different domains of 16S RNA as defined from its primary and secondary structure [20] are also distinct domains in three dimensions, so that the 'body' is made up of the 5' domain of 16S RNA, the 'platform' is made up of the central domain, the 'head' is made up of the 3' major domain, and the terminal 3' minor domain consists of two helices, one of which is the long helix 44 which is responsible for many of the intersubunit contacts. The shape of the subunit is largely conferred by its RNA component, and the junction between the domains is in the central cleft that is the binding site for mRNA and tRNA ligands. The surface of the subunit that interacts with the 50S subunit at the interface consists mostly of RNA, whereas proteins decorate the back (or 'cytoplasmic') side. The structure not only has been used extensively by biochemists and geneticists, but also has been useful in the interpretation of lower-resolution X-ray and EM maps of the ribosome (e.g. [21,22]), and as a molecular-replacement model to phase other crystal structures of the 70S ribosome (e.g. [23]).

At about the same time, another 30S subunit structure at a somewhat lower resolution of 3.3 Å was published [24]. As originally reported, this structure was at considerable variance with the structure reported from our laboratory. As described previously, the registry of several hundred nucleotides of RNA was different, as were the topologies of previously unknown proteins [25]. A subsequent structure from the same group is essentially identical with the one we originally reported, despite only a modest improvement in resolution to 3.1 Å [26], suggesting that most of the earlier discrepancies were due to differences in interpretation of the maps rather than to any genuine variation between the two structures.

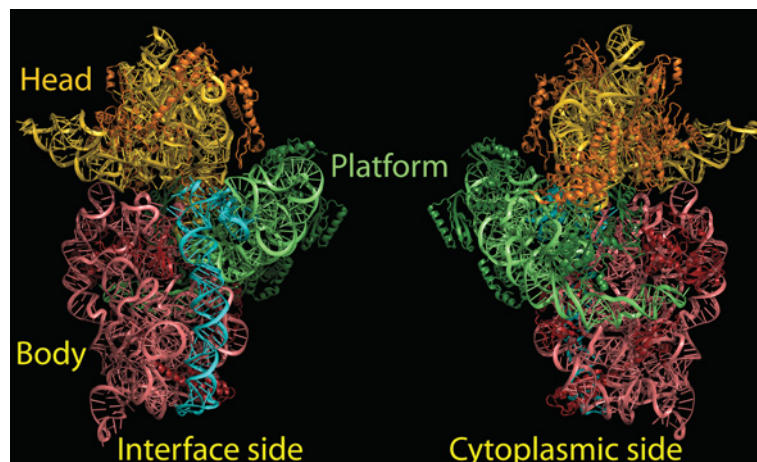
Antibiotic binding

An immediate consequence of the determination of the high-resolution structure of the subunits was the ability to determine the structures of complexes with antibiotics. Thus we reported the structures of streptomycin, paromomycin and spectinomycin bound to the 30S subunit [27] simultaneously with the original 30S structure, and the complexes of tetracycline, hygromycin B and pactamycin soon afterwards [27a]. Several other ribosome–antibiotic structures, notably of several clinically important antibiotics that interact with the peptidyltransferase centre in the 50S subunit, have also been determined elsewhere (e.g. [28–30]).

These structures have shed considerable light on how the antibiotics function. They are also proving useful in the

Figure 1 | The structure of the 30S subunit as determined by crystallography, shown from the front (subunit interface side) and back (cytoplasmic) side

The different domains of 16S RNA in the subunit are coloured salmon (5' domain or body), green (central domain or platform), gold (3' major domain or head) and cyan (3' minor domain). In each case, the protein component of the domain is in a correspondingly darker colour compared with the RNA. The Figure was drawn using PyMOL (DeLano Scientific; <http://www.pymol.org>).



design of novel compounds that might help in the effort to find antibiotics that are effective against multidrug-resistant bacteria [31].

Decoding

Translation is a highly accurate process, and consists of several independent processes which individually need to be at least as accurate as the overall rate of translation. The first involves the recognition of the appropriate tRNA by its aminoacyl synthetase for charging it with the correct amino acid. A second involves maintenance of the reading frame during translation, which is equally crucial. The third, which is of relevance in this work, involves decoding, or the conversion of the information in the codon into its corresponding amino acid during protein synthesis. This in turn involves selection of the appropriate aminoacyl-tRNA through base pairing of the codon on mRNA with the anticodon on the tRNA. This pairing itself has some peculiarities, because ever since the discovery of the genetic code, it has been known that the code is highly degenerate: many codons that differ at the third position code for the same amino acid. The fact that there are fewer tRNAs than there are codons led to the ‘wobble hypothesis’ in which certain kinds of mismatches are tolerated at the third or ‘wobble’ position, whereas strict Watson–Crick pairing is required at the first two positions of the codon [32].

A mismatch in a base pair is not sufficiently discriminating by itself to account for the accuracy of translation. The earliest evidence that the ribosome was involved in the accuracy of tRNA selection came when the antibiotic streptomycin, which binds to the 30S subunit, was found to increase the error rate of protein synthesis [33]. This led to the proposal that the 30S subunit had a decoding centre in which

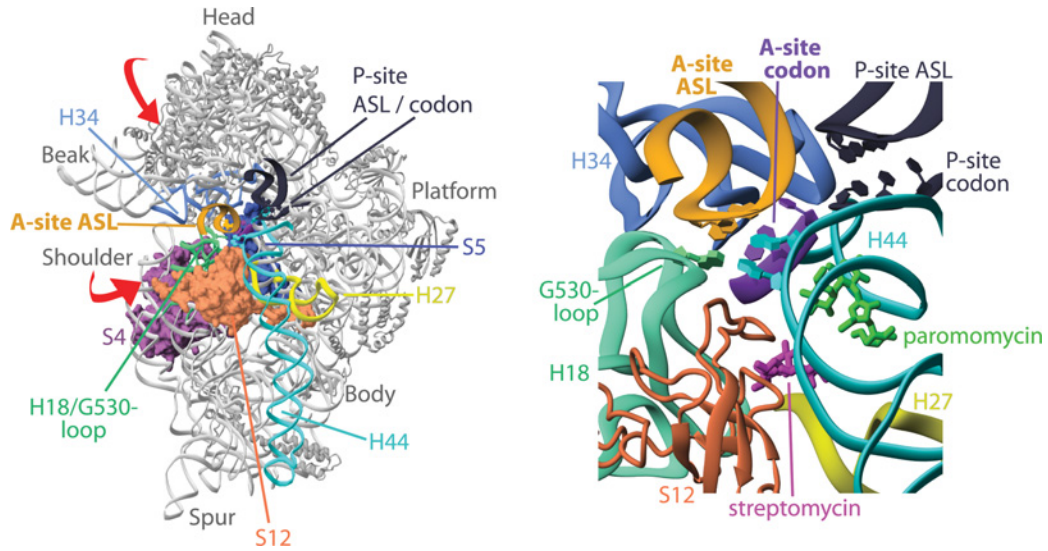
it ‘inspects’ the pairing of codon with anticodon in much the same way that an enzyme senses the precise pairing of its substrate. However, this view of direct inspection ran into difficulties when a mutation, the Hirsh suppressor, was discovered at a location on tRNA that was far from the anticodon [34], which led to the following alternative view.

Aminoacyl-tRNA is initially brought into the ribosome as a complex with EF-Tu and GTP. In a view of decoding termed kinetic proofreading [35,36], incorrect tRNAs can dissociate before and after they are released by EF-Tu, with the overall selectivity being as much as the product of both selection steps. Experimental evidence for proofreading came when it was shown that near-cognate tRNAs (which contain a single subtle mismatch between codon and anticodon) require more GTPs hydrolysed per amino acid incorporated compared with the cognate case [37,38]. In this view, both the ribosome and tRNA were passive participants in translation, with mutations altering accuracy by affecting the rate at which GTP was hydrolysed by EF-Tu. In principle, this could explain how mutations distant from the codon–anticodon pairing could affect accuracy.

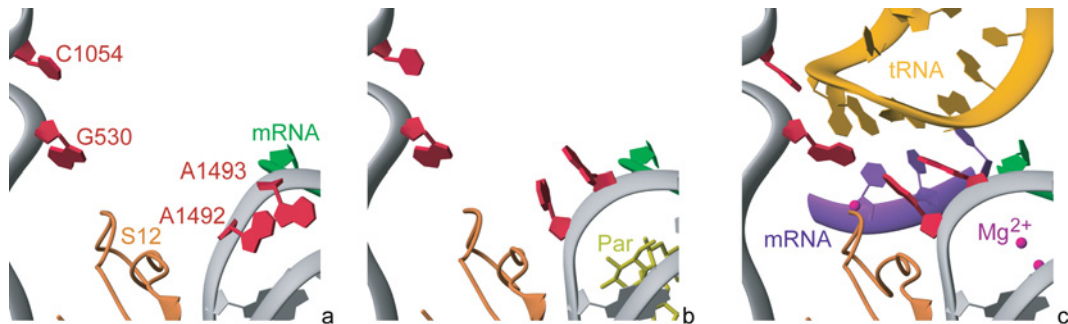
This view has required significant revision. Careful studies on the stability of RNA helices show that the free energy differences from a base-pairing mismatch can account for a factor of 5–10 [39], rather than the factor of 100 assumed previously, showing that, even with proofreading, the accuracy could not be accounted for by base pairing alone. Pre-steady-state kinetic experiments that dissected the various steps in tRNA selection showed that the forward rates of GTPase activation and accommodation (movement of tRNA into the peptidyltransferase centre) were dramatically higher for cognate compared with near-cognate tRNA ([40] and reviewed in [41]). This suggested that cognate tRNA

Figure 2 | The decoding centre of the 30S subunit

Shown is the environment of the decoding centre in the A site, where the tRNA ASL base pairs with the codon of mRNA. Reproduced from [69] with permission.

**Figure 3 | Conformational changes in the decoding centre on antibiotic and tRNA binding**

(a) The decoding centre in the empty 30S subunit. (b) The binding of the antibiotic paromomycin has induced a conformational change in the bases A1492 and A1493, so that they are in a position to interact with the codon–anticodon base pairs. (c) The base pairing between the anticodon of tRNA with the codon induces a change not only in A1492 and A1493, but also in G530 so that all three bases interact with the minor groove of the codon–anticodon mini-helix. Modified from [44] with permission.

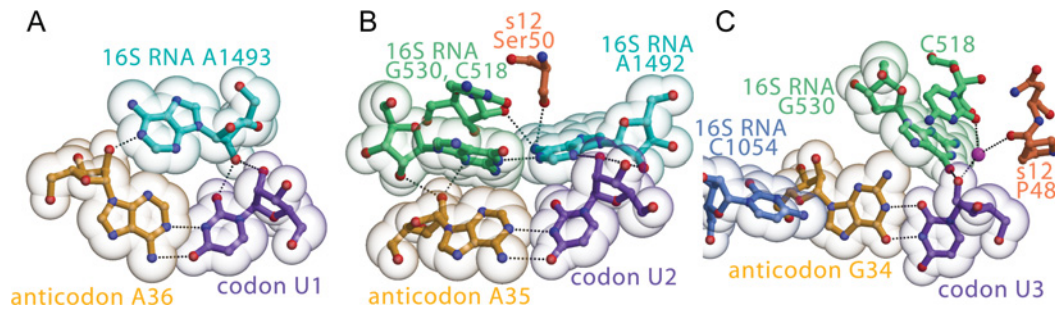


more efficiently induced conformational changes in the ribosome into a productive form that accelerated GTPase activation or accommodation, consistent with earlier suggestions from NMR studies on a portion of the decoding site [42]. Several aminoglycoside antibiotics bind to the decoding centre. These antibiotics also have the effect of increasing the error rate of translation. Kinetic studies showed that a main effect of these antibiotics was less to increase the affinity of incorrect near-cognate tRNAs than to allow such tRNAs to accelerate GTPase activation, presumably by helping to induce the same conformational change that was induced by cognate tRNAs even without the antibiotic.

Possibly one of the most interesting functional insights from the structure of the 30S subunit has come from studies on codon–anticodon interactions at its decoding centre [43]. The decoding site of the 30S subunit is shown in Figure 2. The

structure of the 30S subunit bound to paromomycin showed that the antibiotic resulted in stabilizing the conformation of two key bases, A1492 and A1493, in an orientation in which they would be able to inspect the minor groove of the codon–anticodon helix directly [27] (Figures 3a and 3b). This idea was tested by studying the complex of the 30S subunit with RNA oligonucleotides that mimicked the RNA codon and tRNA ASL (anticodon stem–loop). The data showed that the binding of cognate tRNA to the 30S subunit induced a change in the conformation not only of A1492 and A1493, but also of G530, which is part of the ‘530 pseudoknot’ of 16S RNA (Figure 3c). These three universally conserved bases lined the minor groove of the codon–anticodon helix in such a way that the geometry of the base pair was sensed at the first two positions, but not at the wobble position (Figure 4), thus providing a structural rationale for the wobble hypothesis [32].

Figure 4 | Interaction of conserved ribosomal bases with the three codon–anticodon base pairs showing a specific recognition of Watson–Crick geometry at the first two positions and a tolerance of a GU wobble pair at the third position
Modified from [69] with permission.



The binding of cognate tRNA also induced global conformational changes in the 30S subunit, particularly a movement of the shoulder of the 30S subunit relative to the rest of the body [44,45]. This conformational change was not observed with near-cognate tRNA unless the antibiotic paromomycin was also present. This suggested that the closed form induced by cognate tRNA could also be induced by near-cognate tRNA in the presence of paromomycin. Together, these structures complemented kinetic data which suggested that cognate, but not near-cognate, tRNA induced a conformational change that accelerated the rate of GTP hydrolysis by EF-Tu [40,46].

A further examination of the conformational change showed that many mutations in the 30S that affected accuracy were at or close to an interface between the shoulder and body of the subunit. Mutations that destabilized the open form or antibiotics that stabilized the closed form lowered the accuracy of tRNA selection, and mutations that destabilized the closed form increased the accuracy of tRNA selection [45]. The conformational changes during decoding allowed the rationalization and integration of disparate genetic and biochemical data in terms of a common mechanism [43].

The role of modifications in tRNA during decoding

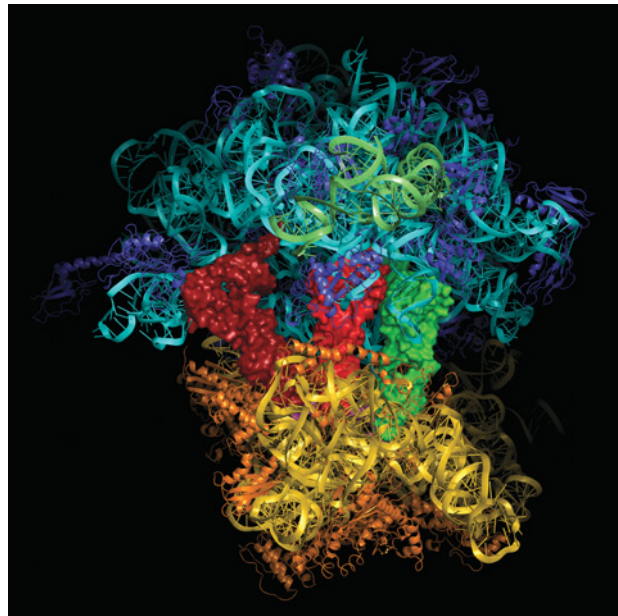
In addition to having proper codon–anticodon base pairing, there are a number of cases where decoding by tRNA requires the specific modification of bases in the anticodon loop. Structures of both lysine and valine tRNA ASLs have shed light on how these modifications might provide additional binding energy to induce the conformational change required for tRNA selection, and also allow a single valine tRNA to decode all four valine codons with the modification, but not without [47,48].

Functional complexes of the 70S ribosome

Interesting as studies on individual subunits are, many of the processes in translation can only be understood in the context of the entire ribosome. Among these are the action of GTPase factors during initiation, elongation and termin-

Figure 5 | Overview of the high-resolution structure of the 70S ribosome complexed with mRNA and tRNA

The structure shows the 50S subunit on top, with the 23S RNA coloured cyan and 5S RNA coloured green. The 50S proteins are shown in dark blue. At the bottom is the 30S subunit, with 16S RNA in gold and the 30S proteins in orange. Nestled between the two subunits are the A-site (green), P-site (red) and E-site (reddish brown) tRNAs. The mRNA at these three sites is just barely visible as a magenta strand. The Figure was drawn using PyMOL (DeLano Scientific; <http://www.pymol.org>).



ation, and the recognition of stop codons and the resultant hydrolysis of the nascent peptide by release factors.

Remarkable strides have been made in determining the structures of a large number of functional complexes by cryo-EM at ever-increasing resolutions [49]. However, the kinds of details seen at the peptidyltransferase centre of the 50S subunit (e.g. [50]) or the decoding centre of the 30S subunit are only obtainable currently with high-resolution crystal structures by crystallography.

Crystals of the whole ribosome were first obtained two decades ago [2], but these initial crystals did not diffract very well [51]. The use of defined mRNA containing a Shine–Dalgarno sequence and defined P- and A-site tRNAs resulted in a structure at 7.8 Å resolution initially [18] and at 5.5 Å resolution 2 years later [22]. By the time of the latter structure, atomic structures of both subunits had been solved, so it was possible to interpret the structure in molecular terms. Although an important landmark, it was not possible at this resolution to accurately model previously unknown features such as the L1 stalk, the L7/L12 stalk, previously unknown proteins such as some in the 50S subunit or some of the intersubunit interface features. Moreover, details of interactions, e.g. with mRNA and tRNA ligands, could only be inferred rather than observed directly, since, at this resolution, the conformation of individual main chains or side chains cannot be seen in sufficient detail.

A second advance in this area came when the structure of an intact, but empty, ribosome was solved to 3.5 Å resolution [23]. Apart from the improved resolution, this structure was significant because it was of the ribosome from *Escherichia coli*, which has for decades been the standard species for studies in biochemistry and genetics, but which was previously thought not to be suitable for ribosome crystallography.

Recently, we solved the structure of the intact 70S ribosome complexed with mRNA and tRNA at 2.8 Å resolution (Figure 5) [52]. At this resolution, one can see directly details of the interaction of the ribosome with its mRNA and tRNA ligands, the nature of the intersubunit interface and also the role of metal ions in the structure. It was also possible to model those proteins from the *Thermus* ribosome that were previously unknown, as well as correct the identification of proteins L28 and L31. A few aspects of the structure are noted below.

A kink in mRNA

The mRNA between the A- and P-site codons has a sharp kink. This deformation of mRNA at the codon boundary has been predicted for at least several decades [53] because, once the structure of tRNA had been solved, it was realized that the two double-helical ASLs could only approach adjacent codons at an angle to avoid a steric clash. The kink was observed in the first crystal structures of functional ribosomal complexes [18,22]. In the high-resolution structure of the 70S ribosome, this kink appears to be stabilized by an Mg²⁺ ion that is also co-ordinated by phosphate oxygens from 16S RNA.

The peptidyltransferase centre

The determination of the structure of the archaeal *H. marismortui* 50S subunit [17] and its complex with a peptidyltransferase inhibitor [54] showed that the active site for catalysis of the peptide bond consisted of RNA, thus finally establishing that catalysis in the ribosome is RNA-based.

The conformation of the peptidyltransferase centre in the bacterial ribosome appears to be very similar to that observed previously in the *Haloarcula* 50S subunit in the presence of

oligonucleotide mimics of tRNA [50]. The suggestion from a recent lower-resolution structure of the 70S ribosome that the peptidyltransferase centre may be significantly different in some complexes of the entire ribosome, as compared with those seen previously in the 50S subunit [55], has been disputed recently on the basis of analysis of both sets of 70S crystallographic data by cross-crystal averaging [56].

An interesting difference with the archaeal 50S subunit structure is that the N-terminal tail of ribosomal protein L27 protrudes into the peptidyltransferase centre where it is in a position to make direct contacts with the CCA end of P-site tRNA (the CCA end of A-site tRNA is disordered in our structure). This protein was known to be cross-linked to the 3'-ends of both A- and P-site tRNAs [57]. Deletion of this protein, or even just the first few N-terminal residues, leads to a reduction in peptidyltransferase activity [58]. The structure suggests that the protein stabilizes the A- and P-site tRNA substrates during peptidyl transfer, thus helping to increase the rate of the reaction. However, since *E. coli* is viable even with the gene for L27 deleted, the protein is unlikely to play a fundamental role in the reaction mechanism, which remains RNA-based and is an example of substrate-assisted catalysis [59].

The E site

In addition to the aminoacyl and peptidyl sites for tRNA, all ribosomes contain an 'exit' or E site [60]. The nature and role of the E-site remains controversial, and, in particular, Nierhaus and his colleagues have suggested that it plays a role in the accuracy of decoding [61] as well as in maintaining the reading frame [62].

It was suggested a long time ago that the reason for the existence of two ribosomal subunits is that they move relative to each other during translocation to form intermediate hybrid states [63]. These hybrid states were established in a series of chemical footprinting experiments, and showed that movement of tRNAs during translocation occurs first with respect to the 50S subunit, resulting in a P/E hybrid tRNA that was bound to the P site in the 30S subunit but the E site in the 50S subunit [64]. The hybrid state has also been suggested as important for facilitating translocation in kinetic studies [65]; in accordance with this, many mutations that affect E-site tRNA binding in the 50S subunit also affect translocation [66,67].

The terminal A76 of E-site tRNA is intercalated between two purines of 23S RNA and makes hydrogen bonds with a universally conserved cytidine in exactly the same way as was seen in the archaeal 50S subunit with a mini-helix tRNA analogue [68]. However, the conformation of the adjacent C75 is very different in the two structures: in the archaeal 50S structure, the base is splayed out from its normal conformation in tRNA and is buried in a pocket formed by a protein (L44e) that is not present in bacteria. These two structures show that, because the crucial interactions with A76 are identical in both, the evolution of the E site must have pre-dated the divergence of archaea and bacteria. However, other features of the E site have apparently been free to

diverge. In any case, the strong conservation of essential structural features between kingdoms confirms the functional importance of the E site suggested by biochemical studies.

Future goals

The high-resolution structures of ribosomal subunits have shed considerable light on specific aspects of ribosome function such as decoding, peptidyltransferase and antibiotic binding. Nevertheless, a large number of major questions about translation remain unanswered. These include the mechanism of action of GTPase factors and release factors, the movement of the ribosome, especially during translocation, and the detailed nature of the various states in the pathway. Finally, a corresponding understanding of eukaryotic translation is still in its infancy. Eukaryotic initiation is highly subject to regulation and involves as many as a dozen factors, some of which are as massive as a ribosomal subunit and consist of almost a dozen subunits. These problems will require years of effort by the community to unravel. However, given the central role of translation in the cell, it seems a worthwhile endeavour.

I am very grateful to the several generations of dedicated and talented students, postdocs and technicians from my laboratory whose contributions I have described here. Work in my laboratory has been funded by the Medical Research Council (U.K.), the National Institutes of Health (U.S.A.), the Agouron Institute, the Louisjeantet Foundation and the Wellcome Trust.

References

- Yonath, A., Müssig, J., Tesche, B., Lorenz, S., Erdmann, V.A. and Wittmann, H.G. (1980) Crystallization of the large ribosomal subunits from *Bacillus stearothermophilus*. *Biochem. Int.* **1**, 428–435
- Trakhanov, S.D., Yusupov, M.M., Agalarov, S.C., Garber, M.B., Ryazantsev, S.N., Tischenko, S.V. and Shirokov, V.A. (1987) Crystallization of 70S ribosomes and 30S ribosomal subunits from *Thermus thermophilus*. *FEBS Lett.* **220**, 319–322
- von Böhlen, K., Makowski, I., Hansen, H.A.S., Bartels, H., Berkovitch-Yellin, Z., Zaytzev-Bashan, A., Meyer, S., Paulke, C., Franceschi, F. and Yonath, A. (1991) Characterization and preliminary attempts for derivatization of crystals of large ribosomal subunits from *Haloarcula marismortui* diffracting to 3 Å resolution. *J. Mol. Biol.* **222**, 11–15
- Holmes, K.C. and Rosenbaum, G. (1998) How X-ray diffraction with synchrotron radiation got started. *J. Synchrotron Radiat.* **5**, 147–153
- Hope, H. (1988) Cryocrystallography of biological macromolecules: a generally applicable method. *Acta Crystallogr. Sect. B Struct. Sci.* **44**, 22–26
- Hope, H., Frolow, F., von Böhlen, K., Makowski, I., Kratky, C., Halfon, Y., Danz, H., Webster, P., Bartels, K.S., Wittmann, H.G. and Yonath, A. (1989) Cryocrystallography of ribosomal particles. *Acta Crystallogr. Sect. B Struct. Sci.* **45**, 190–199
- Ban, N., Freeborn, B., Nissen, P., Penczek, P., Grassucci, R.A., Sweet, R., Frank, J., Moore, P.B. and Steitz, T.A. (1998) A 9 Å resolution x-ray crystallographic map of the large ribosomal subunit. *Cell* **93**, 1105–1115
- Schlunzen, F., Hansen, H.A.S., Thygesen, J., Bennett, W.S., Volkman, N., Levin, I., Harms, J., Bartels, H., Zaytzev-Bashan, A., Berkovitch-Yellin, Z. et al. (1995) A milestone in ribosomal crystallography: the construction of preliminary electron density maps at intermediate resolution. *Biochem. Cell Biol.* **73**, 739–749
- Clemons, Jr, W.M., Brodersen, D.E., McCutcheon, J.P., May, J.L., Carter, A.P., Morgan-Warren, R.J., Wimberly, B.T. and Ramakrishnan, V. (2001) Crystal structure of the 30S ribosomal subunit from *Thermus thermophilus*: purification, crystallization and structure determination. *J. Mol. Biol.* **310**, 827–843
- Ramakrishnan, V. and Biou, V. (1997) Treatment of multiwavelength anomalous diffraction data as a special case of multiple isomorphous replacement. *Methods Enzymol.* **276**, 538–557
- Ramakrishnan, V., Finch, J.T., Graziano, V., Lee, P.L. and Sweet, R.M. (1993) Crystal structure of globular domain of histone H5 and its implications for nucleosome binding. *Nature* **362**, 219–223
- Hendrickson, W.A., Horton, J.R. and LeMaster, D.M. (1990) Selenomethionyl proteins produced for analysis by multiwavelength anomalous diffraction (MAD): a vehicle for direct determination of three-dimensional structure. *EMBO J.* **9**, 1665–1672
- Weis, W.I., Kahn, R., Fourme, R., Drickamer, K. and Hendrickson, W.A. (1991) Structure of the calcium-dependent lectin domain from a rat mannose-binding protein determined by MAD phasing. *Science* **254**, 1608–1615
- Cate, J.H., Gooding, A.R., Podell, E., Zhou, K., Golden, B.L., Kundrot, C.E., Cech, T.R. and Doudna, J.A. (1996) Crystal structure of a group I ribozyme domain: principles of RNA packing. *Science* **273**, 1678–1685
- Clemons, Jr, W.M., May, J.L., Wimberly, B.T., McCutcheon, J.P., Capel, M.S. and Ramakrishnan, V. (1999) Structure of a bacterial 30S ribosomal subunit at 5.5 Å resolution. *Nature* **400**, 833–840
- Terwilliger, T. and Berendzen, J. (1999) Automated MAD and MIR structure determination. *Acta Crystallogr. Sect. D Biol. Crystallogr.* **55**, 849–861
- Ban, N., Nissen, P., Hansen, J., Moore, P.B. and Steitz, T.A. (2000) The complete atomic structure of the large ribosomal subunit at 2.4 Å resolution. *Science* **289**, 905–920
- Cate, J.H., Yusupov, M.M., Yusupova, G.Z., Earnest, T.N. and Noller, H.F. (1999) X-ray crystal structures of 70S ribosome functional complexes. *Science* **285**, 2095–2104
- Wimberly, B.T., Brodersen, D.E., Clemons, Jr, W.M., Morgan-Warren, R.J., Carter, A.P., Vornrhein, C., Hartsch, T. and Ramakrishnan, V. (2000) Structure of the 30S ribosomal subunit. *Nature* **407**, 327–339
- Noller, H.F. and Woese, C.R. (1981) Secondary structure of 16S ribosomal RNA. *Science* **212**, 403–411
- Gao, H., Sengupta, J., Valle, M., Korostelev, A., Eswar, N., Stagg, S.M., Van Roey, P., Agrawal, R.K., Harvey, S.C., Sali, A. et al. (2003) Study of the structural dynamics of the *E. coli* 70S ribosome using real-space refinement. *Cell* **113**, 789–801
- Yusupov, M.M., Yusupova, G.Z., Baucom, A., Lieberman, K., Earnest, T.N., Cate, J.H. D. and Noller, H.F. (2001) Crystal structure of the ribosome at 5.5 Å resolution. *Science* **292**, 883–896
- Schuwirth, B.S., Borovinskaya, M.A., Hau, C.W., Zhang, W., Vila-Sanjurjo, A., Holton, J.M. and Cate, J.H. (2005) Structures of the bacterial ribosome at 3.5 Å resolution. *Science* **310**, 827–834
- Schlunzen, F., Tocilj, A., Zarivach, R., Harms, J., Gluehmann, M., Janell, D., Bashan, A., Bartels, H., Agmon, I., Franceschi, F. and Yonath, A. (2000) Structure of functionally activated small ribosomal subunit at 3.3 angstroms resolution. *Cell* **102**, 615–623
- Brodersen, D.E., Clemons, Jr, W.M., Carter, A.P., Wimberly, B.T. and Ramakrishnan, V. (2002) Crystal structure of the 30S ribosomal subunit from *Thermus thermophilus*: structure of the proteins and their interactions with 16S RNA. *J. Mol. Biol.* **316**, 725–768
- Pioletti, M., Schlunzen, F., Harms, J., Zarivach, R., Gluehmann, M., Avila, H., Bashan, A., Bartels, H., Auerbach, T., Jacobi, C. et al. (2001) Crystal structures of complexes of the small ribosomal subunit with tetracycline, edeine and IF3. *EMBO J.* **20**, 1829–1839
- Carter, A.P., Clemons, Jr, W.M., Brodersen, D.E., Morgan-Warren, R.J., Wimberly, B.T. and Ramakrishnan, V. (2000) Functional insights from the structure of the 30S ribosomal subunit and its interactions with antibiotics. *Nature* **407**, 340–348
- Brodersen, D.E., Clemons, Jr, W.M., Carter, A.P., Morgan-Warren, R.J., Wimberly, B.T. and Ramakrishnan, V. (2000) The structural basis for the action of the antibiotics tetracycline, pactamycin, and hygromycin B on the 30S ribosomal subunit. *Cell* **103**, 1143–1154
- Schlunzen, F., Zarivach, R., Harms, R., Bashan, A., Tocilj, A., Albrecht, R., Yonath, A. and Franceschi, F. (2001) Structural basis for the interaction of antibiotics with the peptidyl transferase centre in eubacteria. *Nature* **413**, 814–821

- 29 Hansen, J.L., Moore, P.B. and Steitz, T.A. (2003) Structures of five antibiotics bound at the peptidyl transferase center of the large ribosomal subunit. *J. Mol. Biol.* **330**, 1061–1075
- 30 Tu, D., Blaha, G., Moore, P.B. and Steitz, T.A. (2005) Structures of MLSBK antibiotics bound to mutated large ribosomal subunits provide a structural explanation for resistance. *Cell* **121**, 257–270
- 31 Franceschi, F. and Duffy, E.M. (2006) Structure-based drug design meets the ribosome. *Biochem. Pharmacol.* **71**, 1016–1025
- 32 Crick, F.H.C. (1966) Codon–anticodon pairing: the wobble hypothesis. *J. Mol. Biol.* **19**, 548–555
- 33 Davies, J., Gilbert, W. and Gorini, L. (1964) Streptomycin, suppression, and the code. *Proc. Natl. Acad. Sci. U.S.A.* **51**, 883–890
- 34 Hirsh, D. (1971) Tryptophan transfer RNA as the UGA suppressor. *J. Mol. Biol.* **58**, 439–458
- 35 Hopfield, J.J. (1974) Kinetic proofreading: a new mechanism for reducing errors in biosynthetic processes requiring high specificity. *Proc. Natl. Acad. Sci. U.S.A.* **71**, 4135–4139
- 36 Ninio, J. (1975) Kinetic amplification of enzyme discrimination. *Biochimie* **57**, 587–595
- 37 Thompson, R.C. and Stone, P.J. (1977) Proofreading of the codon–anticodon interaction on ribosomes. *Proc. Natl. Acad. Sci. U.S.A.* **74**, 198–202
- 38 Ruusala, T., Ehrenberg, M. and Kurland, C.G. (1982) Is there proofreading during polypeptide synthesis? *EMBO J.* **1**, 741–745
- 39 Sugimoto, N., Kierzek, R., Freier, S.M. and Turner, D.H. (1986) Energetics of internal GU mismatches in ribooligonucleotide helices. *Biochemistry* **25**, 5755–5759
- 40 Pape, T., Wintermeyer, W. and Rodnina, M.V. (1999) Induced fit in initial selection and proofreading of aminoacyl-tRNA on the ribosome. *EMBO J.* **18**, 3800–3807
- 41 Rodnina, M.V. and Wintermeyer, W. (2001) Fidelity of aminoacyl-tRNA selection on the ribosome: kinetic and structural mechanisms. *Annu. Rev. Biochem.* **70**, 415–435
- 42 Fourmy, D., Yoshizawa, S. and Puglisi, J.D. (1998) Paromomycin binding induces a local conformational change in the A-site of 16S rRNA. *J. Mol. Biol.* **277**, 333–345
- 43 Ogle, J.M. and Ramakrishnan, V. (2005) Structural insights into translational fidelity. *Annu. Rev. Biochem.* **74**, 129–177
- 44 Ogle, J.M., Brodersen, D.E., Clemons, Jr, W.M., Tarry, M.J., Carter, A.P. and Ramakrishnan, V. (2001) Recognition of cognate transfer RNA by the 30S ribosomal subunit. *Science* **292**, 897–902
- 45 Ogle, J.M., Murphy, F.V., Tarry, M.J. and Ramakrishnan, V. (2002) Selection of tRNA by the ribosome requires a transition from an open to a closed form. *Cell* **111**, 721–732
- 46 Pape, T., Wintermeyer, W. and Rodnina, M.V. (2000) Conformational switch in the decoding region of 16S rRNA during aminoacyl-tRNA selection on the ribosome. *Nat. Struct. Biol.* **7**, 104–107
- 47 Murphy, F.V., Ramakrishnan, V., Malkiewicz, A. and Agris, P.F. (2004) The role of modifications in codon discrimination by tRNA(Lys)UUU. *Nat. Struct. Mol. Biol.* **11**, 1186–1191
- 48 Weixlbaumer, A., Murphy, F.V., Dziergowska, A., Malkiewicz, A., Vendeix, F.A., Agris, P.F. and Ramakrishnan, V. (2007) Mechanism for expanding the decoding capacity of transfer RNAs by modification of uridines. *Nat. Struct. Mol. Biol.* **14**, 498–502
- 49 Mitra, K. and Frank, J. (2006) Ribosome dynamics: insights from atomic structure modeling into cryo-electron microscopy maps. *Annu. Rev. Biophys. Biomol. Struct.* **35**, 299–317
- 50 Schmeing, T.M., Huang, K.S., Strobel, S.A. and Steitz, T.A. (2005) An induced-fit mechanism to promote peptide bond formation and exclude hydrolysis of peptidyl-tRNA. *Nature* **438**, 520–524
- 51 Trakhanov, S., Yusupov, M., Shirokov, V., Garber, M., Mitschler, A., Ruff, M., Thierry, J.C. and Moras, D. (1989) Preliminary X-ray investigation of 70 S ribosome crystals from *Thermus thermophilus*. *J. Mol. Biol.* **209**, 327–328
- 52 Selmer, M., Dunham, C.M., Murphy, F.V., Weixlbaumer, A., Petry, S., Kelley, A.C., Weir, J.R. and Ramakrishnan, V. (2006) Structure of the 70S ribosome complexed with mRNA and tRNA. *Science* **313**, 1935–1942
- 53 Rich, A. (1974) How transfer RNA may move. in *Ribosomes* (Nomura, M., Tissières, A. and Lengyel, P., eds.), pp. 871–884, Cold Spring Harbor Laboratory Press, Cold Spring Harbor
- 54 Nissen, P., Hansen, J., Ban, N., Moore, P.B. and Steitz, T.A. (2000) The structural basis of ribosome activity in peptide bond synthesis. *Science* **289**, 920–930
- 55 Korostelev, A., Trakhanov, S., Laurberg, M. and Noller, H.F. (2006) Crystal structure of a 70S ribosome–tRNA complex reveals functional interactions and rearrangements. *Cell* **126**, 1065–1077
- 56 Simonovic, M. and Steitz, T.A. (2008) Cross-crystal averaging reveals that the structure of the peptidyl-transferase center is the same in the 70S ribosome and the 50S subunit. *Proc. Natl. Acad. Sci. U.S.A.* **105**, 500–505
- 57 Wower, J., Kirillov, S.V., Wower, I.K., Guven, S., Hixson, S.S. and Zimmermann, R.A. (2000) Transit of tRNA through the *Escherichia coli* ribosome: cross-linking of the 3' end of tRNA to specific nucleotides of the 23S ribosomal RNA at the A, P, and E sites. *J. Biol. Chem.* **275**, 37887–37894
- 58 Maguire, B.A., Beniaminov, A.D., Ramu, H., Mankin, A.S. and Zimmermann, R.A. (2005) A protein component at the heart of an RNA machine: the importance of protein L27 for the function of the bacterial ribosome. *Mol. Cell* **20**, 427–435
- 59 Weinger, J.S., Parnell, K.M., Dorner, S., Green, R. and Strobel, S.A. (2004) Substrate-assisted catalysis of peptide bond formation by the ribosome. *Nat. Struct. Mol. Biol.* **11**, 1101–1106
- 60 Rheinberger, H.J., Sternbach, H. and Nierhaus, K.H. (1981) Three tRNA binding sites on *Escherichia coli* ribosomes. *Proc. Natl. Acad. Sci. U.S.A.* **78**, 5310–5314
- 61 Rheinberger, H.J. and Nierhaus, K.H. (1986) Allosteric interactions between the ribosomal transfer RNA-binding sites A and E. *J. Biol. Chem.* **261**, 9133–9139
- 62 Marquez, V., Wilson, D.N., Tate, W.P., Triana-Alonso, F. and Nierhaus, K.H. (2004) Maintaining the ribosomal reading frame: the influence of the E site during translational regulation of release factor 2. *Cell* **118**, 45–55
- 63 Bretscher, M.S. (1968) Translocation in protein synthesis: a hybrid structure model. *Nature* **218**, 675–677
- 64 Moazed, D. and Noller, H.F. (1989) Intermediate states in the movement of transfer RNA in the ribosome. *Nature* **342**, 142–148
- 65 Semenkov, Y.P., Rodnina, M.V. and Wintermeyer, W. (2000) Energetic contribution of tRNA hybrid state formation to translocation catalysis on the ribosome. *Nat. Struct. Biol.* **7**, 1027–1031
- 66 Lill, R., Robertson, J.M. and Wintermeyer, W. (1989) Binding of the 3' terminus of tRNA to 23S rRNA in the ribosomal exit site actively promotes translocation. *EMBO J.* **8**, 3933–3938
- 67 Feinberg, J.S. and Joseph, S. (2001) Identification of molecular interactions between P-site tRNA and the ribosome essential for translocation. *Proc. Natl. Acad. Sci. U.S.A.* **98**, 11120–11125
- 68 Schmeing, T.M., Moore, P.B. and Steitz, T.A. (2003) Structures of deacylated tRNA mimics bound to the E site of the large ribosomal subunit. *RNA* **9**, 1345–1352
- 69 Ogle, J.M., Carter, A.P. and Ramakrishnan, V. (2003) Insights into the decoding mechanism from recent ribosome structures. *Trends Biochem. Sci.* **28**, 259–266

Received 21 April 2008
doi:10.1042/BST0360567